1

Rapidly Solidified Magnetic Nanowires and Submicron Wires

Tibor-Adrian Óvári, Nicoleta Lupu and Horia Chiriac
National Institute of Research and Development for Technical Physics Iaşi
Romania

1. Introduction

Magnetically soft amorphous glass-coated microwires are suitable for numerous sensor applications. Their typical dimensions – metallic nucleus diameter of 1 to 50 μm and glass coating thickness of 1 to 30 μm – make them promising candidates for high frequency applications, especially given their sensitive giant magneto-impedance (GMI) response in the MHz and GHz ranges (Torrejón et al, 2009). The magnetic properties of amorphous microwires are determined by composition, which gives the sign and magnitude of their magnetostriction, as well as by dimensions – metallic nucleus diameter, glass coating thickness, and their ratio – which are extremely relevant for the level of internal stresses induced during preparation. The magneto-mechanical coupling between internal stresses and magnetostriction is mainly responsible for the distribution of anisotropy axes and domain structure formation. Microwires generally display a core-shell domain structure in their metallic nucleus, with orthogonal easy axes, e.g. axial in the core and circumferential or radial in the shell, as schematically shown in Fig. 1.

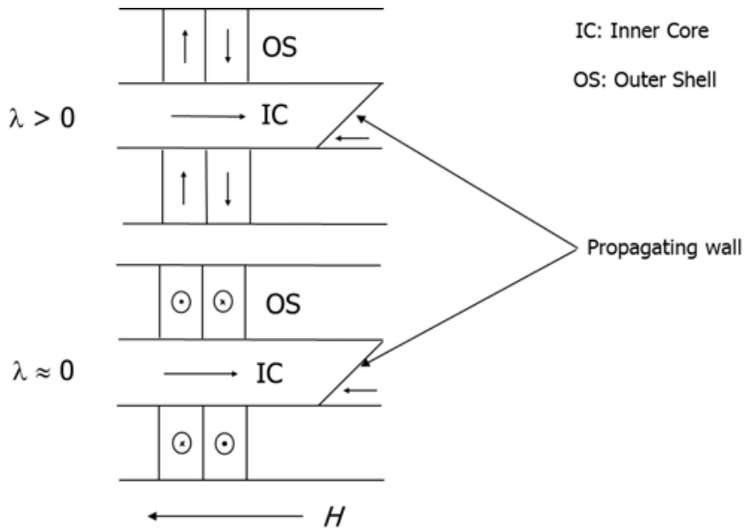

Fig. 1. Typical core-shell domain structures in amorphous glass-coated microwires with positive (λ >0) and nearly zero magnetostriction (λ ≈ 0), respectively.

An axially magnetized core, usually encountered in amorphous microwires with large and positive magnetostriction, but also in nearly zero magnetostrictive ones if their nucleus diameter is larger than 20 μm (Chiriac et al., 2007a), leads to the appearance of the large Barkhausen effect (LBE), that is a single step reversal of the magnetization in the core when the sample is subjected to a small axial magnetic field. LBE takes place through the propagation of a pre-existent 180° domain wall from one microwire end to the other, as illustrated in Fig. 1.

Ferromagnetic nanowires are aimed for novel spintronic applications such as racetrack memory, magnetic domain wall logic devices, domain wall diodes and oscillators, and devices based on field or spin-current torque driven domain wall motion (Allwood et al., 2005; Finocchio et al., 2010; Lee et al., 2007; Parkin et al., 2008). These applications require nanowires with characteristics that can be accurately controlled and tailored, and with large domain wall velocities, since the device speed depends on domain wall velocity. At present, spintronic applications which require magnetic nanowires are based on planar nanowires prepared by expensive lithographic methods (Moriya et al., 2010).

Recently, the large values of domain wall velocity reported in amorphous glass-coated microwires have offered new prospects for the use of these much cheaper rapidly solidified materials in spintronic applications, subject to a significant reduction in their diameter (Chiriac et al., 2009a). The amorphous nanowires are composite materials consisting of a metallic nucleus embedded in a glass coating prepared in a single stage process, the glass-coated melt spinning, at sample lengths of the order of 10^4 m (Chiriac & Óvári, 1996). In order to overcome the experimental difficulties related to the fabrication of such ultra-thin wires and to drastically reduce the typical transverse dimensions of microwires (1 to 50 μm for the metallic nucleus diameter), the apparatus used for the preparation of the rapidly solidified nanowires has been significantly modified. These efforts have led to the successful preparation and characterization of rapidly solidified submicron wires with the metallic nucleus diameter of 800 nm, reported less than 2 years ago (Chiriac et al., 2010). Figure 2 (a) shows the SEM images of a submicron amorphous wire with the nucleus diameter of 800 nm, whilst Fig. 2 (b) illustrates the optical microscopy image of the submicron amorphous wire in comparison with two typical amorphous microwires with the nucleus diameters of 4.7 and 1.8 μm, respectively. These results have opened up the opportunity to develop nanosized rapidly solidified amorphous magnetic materials for applications based on the domain wall motion.

This first success has been shortly followed by the preparation and characterization of amorphous glass-coated submicron wires with metallic nucleus diameters down to 350 nm (Chiriac et al., 2011a), in which domain wall velocity measurements have also shown very promising results (Óvári et al., 2011).

The well-known methods employed in the experimental studies have been extensively modified in order to allow one to perform complex measurements on such thin wires, especially due to the high sensitivity required to measure a single rapidly solidified ultra-thin wire (Corodeanu et al., 2011a).

Following the same path, we have been able to produce rapidly solidified amorphous nanowires through an improved technique. The diameters of the as-quenched nanowires were ranging from 90 to 180 nm (Chiriac et al., 2011b). These new materials are useful for

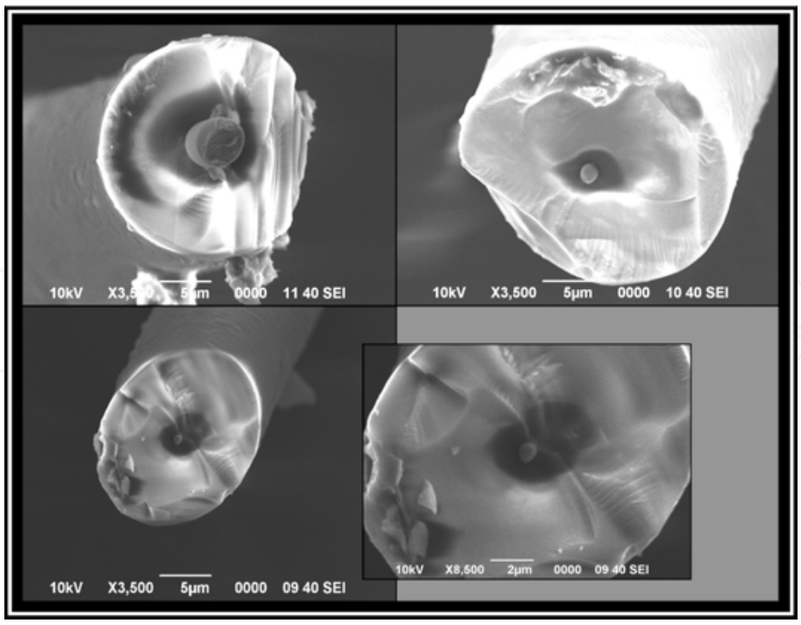

Fig. 2a. SEM images of a submicron amorphous wire with the nucleus diameter of 800 nm.

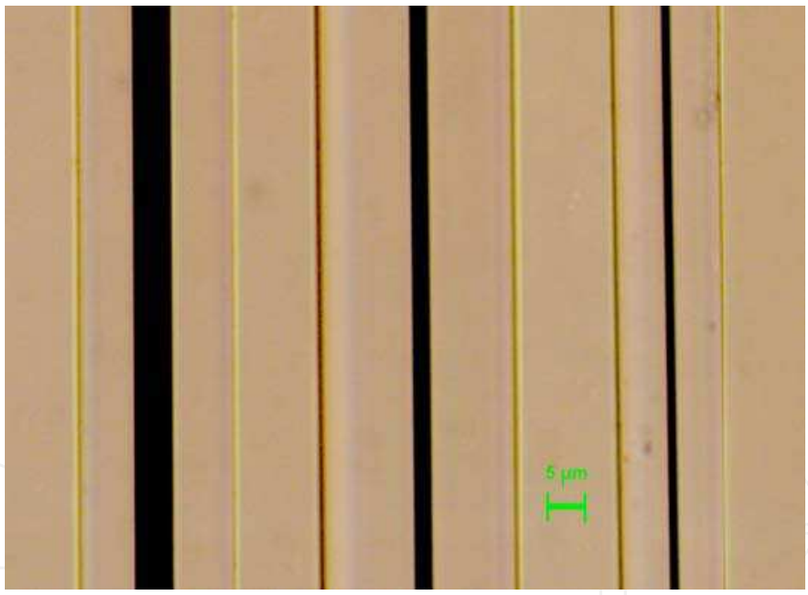

Fig. 2b. Optical microscopy images of the submicron amorphous wire in comparison with two typical amorphous microwires with the nucleus diameters of 4.7 and 1.8 μm, respectively.

applications in both domain wall logic type devices and in novel, miniature sensors. The accurate control of the domain wall motion could be performed without irreversible modifications of the wire geometry, as recently pointed out (Vázquez et al., 2012). Nevertheless, there are several issues to be addressed before these new materials can reach their full practical potential: their integration in electronic circuits, the use of lithographic methods to prepare the miniature coils required to inject and trap domain walls, the clarification of the role of glass coating and whether or not it should be kept, removed or just

partially removed – and in which stages of the device development, issues related to the manipulation of wires with such small diameters, etc.

Figure 3 shows two SEM micrographs of a glass-coated $Fe_{77.5}Si_{7.5}B_{15}$ amorphous magnetic nanowire with the metallic nucleus diameter of 90 nm and the glass coating of 5.5 μm, taken at different magnifications.

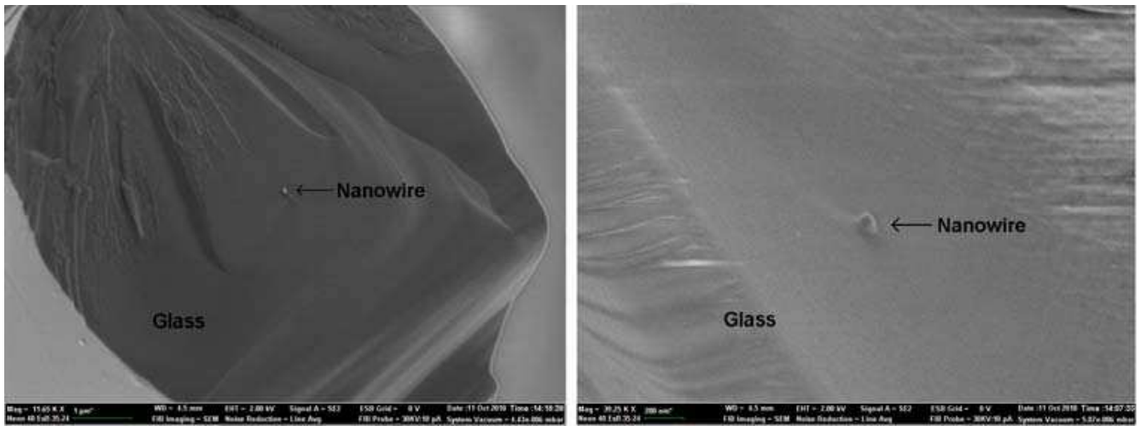

Fig. 3. SEM micrographs at two different magnifications of a rapidly solidified amorphous nanowire with positive magnetostriction having the metallic nucleus diameter of 90 nm and a glass coating thickness of 5.5 μm.

A new method for measuring the domain wall velocity in a single, ultrathin ferromagnetic amorphous wire with the diameter down to 100 nm has been developed in order to measure such novel nanowires (Corodeanu et al., 2011b). The method has been developed in order to increase the sensitivity in studying the domain wall propagation in bistable magnetic wires in a wide range of field amplitudes, with much larger values of the applied field as compared to those employed when studying the wall propagation in typical amorphous microwires. The newly developed method is especially important now, when large effort is devoted to the development of domain wall logic devices based on ultrathin magnetic wires and nanowires.

Besides the spintronic applications, the investigation of rapidly solidified amorphous submicron wires and nanowires is aimed towards the understanding of the changes in the magnetic domain structure, which makes the bistable behavior possible, and in the switching field, at submicron level and at nanoscale.

2. Experimental techniques for the characterization of rapidly solidified amorphous nanowires and submicron wires. Domain wall velocity measurements

2.1 Magnetic characterization

Given the ultra-small diameters of rapidly solidified submicron wires and nanowires (metallic nucleus diameters between several tens of nanometers and hundreds of nanometers), the use of the classical characterization techniques employed for typical microwires with diameters between 1 and 50 μm (Butta et al., 2009; Kulik et al., 1993) in order to measure their basic magnetic properties, e.g. to determine their magnetic hysteresis

loops, is not viable due to the low sensitivity and signal-to-noise ratio (SNR). Therefore, in order to investigate the magnetic properties of a single ultrathin magnetic wire, a reliable measuring system has been developed (Corodeanu et al., 2011a). The new procedure has been employed to measure a single ultrathin magnetic wire, i.e. a submicron wire or a nanowire, using a digital integration technique. The new experimental set-up has been developed in order to increase the sensitivity and to extract from the noisy signal a reliable low frequency hysteresis loop for a single submicron wire or nanowire.

The main components of the measuring system used in the experiments are: the magnetizing solenoid, the system of pick-up coils, a low-noise preamplifier, a function generator, and a data acquisition board. A schematic of the system is shown in Fig. 4.

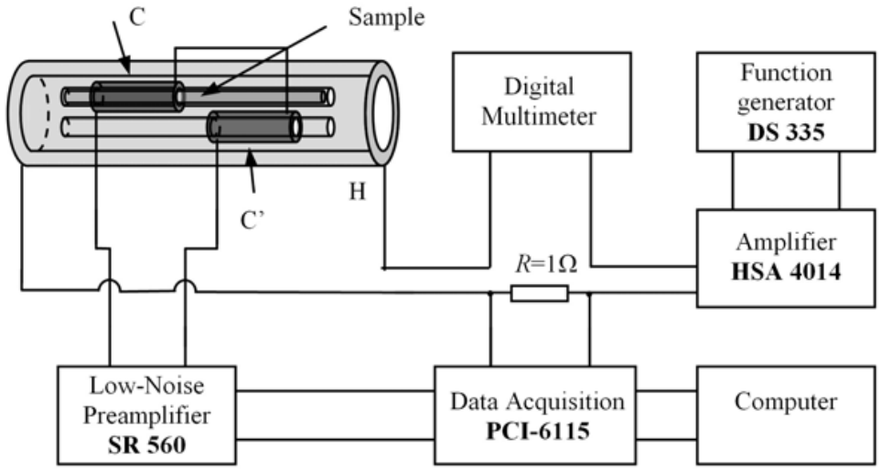

Fig. 4. Schematic of the experimental system employed for the magnetic characterization of rapidly solidified amorphous nanowires and submicron wires.

The magnetizing solenoid is powered by a Stanford Research DS 335 function generator through a high power bipolar amplifier HSA 4014, being capable of generating magnetic fields up to 30,000 A/m. Two pick-up coils connected in series-opposition are used in order to avoid any induced voltage in the absence of the sample. Each pick-up coil is 1 cm long and has 1,570 turns, wound with enameled 0.07 mm copper wire on a ceramic tube with an outer diameter of 1.8 mm and an inner diameter of 1 mm. A 1 Ω resistor (R) is used to provide a voltage proportional to the applied magnetic field. The voltage induced in the pick-up coil is amplified up to 50,000 times using a Stanford Research SR560 low-noise preamplifier in order to obtain a measurable value of the induced voltage and a high SNR. The voltage drop on the resistor R and the amplified induced voltage from the pick-up coil system are digitized using a National Instruments PCI-6115 four channels simultaneous data acquisition board. The acquisition of the signals was done using a sampling frequency between 800 kHz and 10 MHz (with 5,000 to 62,500 points/loop at 160 Hz). The acquired signals have been processed using LabVIEW based software.

Two methods have been employed to measure the hysteresis loops. For the first one, it was necessary to make an average over a large number of acquired signals, while for the second one only two recordings of the signal were required (with and without the sample), followed by digital processing to trace the hysteresis loop.

For the first method, in order to extract the useful signal from the noisy one, two sets of data have been acquired. First, the signal from the pick-up coil system with no sample in it has been acquired; this 'zero signal' contains information about any possible miss-compensation of the pick-up coils either due to the imperfect winding of the pick-up coils or of the magnetizing solenoid. It is necessary to mention at this point that the field generated by the magnetizing solenoid cannot be perfectly uniform. The non-uniformity of the field together with the imperfections in the winding of the pick-up coils will affect the shape of the small induced signal. This effect of the measuring system on the induced signal has to be removed in order to obtain the clearest possible signal from the sample. Subsequently, the induced signal has been digitally integrated, and the integrated signal was averaged over a large number of measurements. In this way, an apparent hysteresis loop of the system with no sample was recorded. An external trigger has been used to avoid any phase mismatch when averaging.

Averaging was done over the integrated signals rather than the induced signals. This was due to the very small width of the peaks (of the order of 10 μs) in the induced signals, as well as due to the fact that they were not always in the exact same place (magnetization reversal does not always occur at the same value of the field). Averaging such signals would cancel the sample signal together with the noise.

The next step was to insert the sample, using a glass capillary, inside one of the pick-up coils, taking care to avoid any displacements of the coils within the system. The induced signals have been measured again. The corresponding signals were integrated and the integrated signal was averaged as in the previous case in order to obtain the apparent loop of the system with the sample.

The intrinsic hysteresis loop of the sample is obtained in this method by subtracting the apparent loop without the sample from the apparent loop with the sample. A low pass filter has been employed for further noise reduction, taking care not to alter the shape of the sample peaks.

The magnetization process of these materials results in a square hysteresis loop since the magnetization reversal takes place in a single step. Therefore, the induced signal displays a peak, and should be null in rest (zero induced signal since magnetization does not change). Based on this, a second, faster method is proposed to obtain a less noisy hysteresis loop.

In this second method, the signals induced with and without sample are acquired only once. The signal without sample is subtracted from the signal with sample. The SNR is still too small to obtain a good integration. Therefore, a window method has been employed (Butta et al., 2009). Considering that everything outside the peak area of the signal must be zero, two windows were used to select the peak area from the sample signal while the rest of the noisy signal was numerically forced to become null. Using digital integration of the windowed signal and an accurate selection of the peaks, the hysteresis loop of the sample is obtained.

First, a wider range which includes the peak area is selected. The hysteresis loop which corresponds to this selection displays a noisy jump in magnetization, as if the sample magnetization values would be larger and then smaller than the actual values. Therefore, the selection range is progressively reduced in several steps, with integration being performed at each step, in order to reduce the noise as much as possible in the region of the magnetization jump. Special care was taken to avoid cutting the peaks. The selection accuracy does not affect

the measured value of coercivity and only slightly influences the magnetization (less than 5% for the thinnest sample which has been used in the experiments).

Figure 5 shows the hysteresis loops of the same nanowire obtained through both methods.

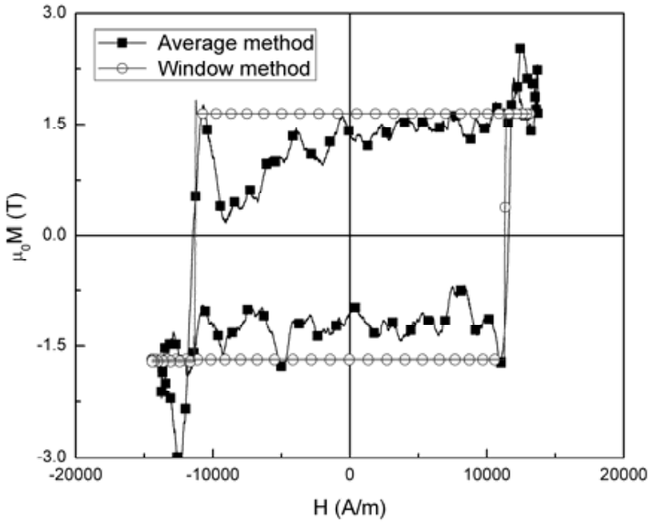

Fig. 5. Hysteresis loop of a 133 nm $Fe_{77.5}Si_{7.5}B_{15}$ nanowire covered by 6 μm of glass measured using both methods (averaged and window).

Thus, a reliable method for the precise magnetic measurement of ultrathin wire shaped samples, e.g. single nanowire, has been developed. The combination of the two methods proposed for hysteresis loop measurements leads to an accurate characterization of materials such as submicron wires and nanowires with diameters down to 100 nm: the first method provides information about the profile of the hysteresis loop and magnetic behavior of the sample (bistable or not), while the second one removes almost all the noise resulting in a valid noise-free loop.

2.2 Domain wall velocity measurements

Magnetic bistability is one of the key characteristics of amorphous glass-coated submicron wires and nanowires which make them important for applications. The magnetic bistable behavior represents the one-step reversal of the magnetization along such samples at a certain value of the applied magnetic field, value which is called switching field (Komova et al., 2008). The actual reversal consists in the displacement of a 180° domain wall along the entire length of the sample. The characteristics of the wall propagation, especially its velocity, are essential for the properties of the domain wall logic devices which could be developed. Therefore, it is extremely important to measure the domain wall velocity and its field dependence with high accuracy, in order to determine the wall mobility and to correctly predict characteristics such as operating speed of the future devices.

Therefore, the development of a new method for measuring the domain wall velocity in a single magnetic wire with dimensions ranging from those of a typical microwire (1 – 50 μm) to those of a submicron wire (hundreds of nm) and further down to a nanowire (100 nm) was required. Such a method was also necessary due to the increment of the field range in

which the wall velocity needs to be measured. The new experimental set-up was developed in order to increase the sensitivity and to study the domain wall mobility and damping mechanisms in bistable magnetic wires in a wide range of the applied field amplitude.

The main problem addressed with the proposed method of measuring the domain wall velocity is related to two important factors which change drastically as the wire diameter decreases from the range of microns to that of submicrons and further down to nanometers: the wall velocity values are very large and the propagation fields become extremely large. Due to these two reasons, the existing measuring methods are inefficient in providing accurate values for the domain wall velocity, mainly due to the nucleation of additional domain walls which propagate among the pick-up coils, rendering the whole measurement incorrect.

The measurement of the domain wall velocity is based on the classical method developed by Sixtus and Tonks (Sixtus & Tonks, 1932). The original method has been improved by various authors, e.g. (Hudak et al., 2009), in order to study the wall propagation in different types of materials under various circumstances. A schematic diagram of the new experimental set-up proposed in this work is shown in figure 6. The experimental set-up consists of a long solenoid (37 cm long, 2 cm in diameter, 2335 turns with a field to current constant of 6214 Am^{-1}/A) powered by a Stanford Research Systems DS 335 function generator through a high power bipolar amplifier HSA 4014, and two compensated systems of four pick-up coils placed within the solenoid. Each pick-up coil system consists of four identical coils *Cx* and *Cx*′ (x = 1, 2, 3, 4) connected in series-opposition in order to obtain a compensated system able to provide only the sample signal and almost zero signal in the absence of the sample. The compensation is especially important for measurements performed on submicron wires and nanowires due to the small sample induced signal relative to the field induced one in the case of non-compensated systems.

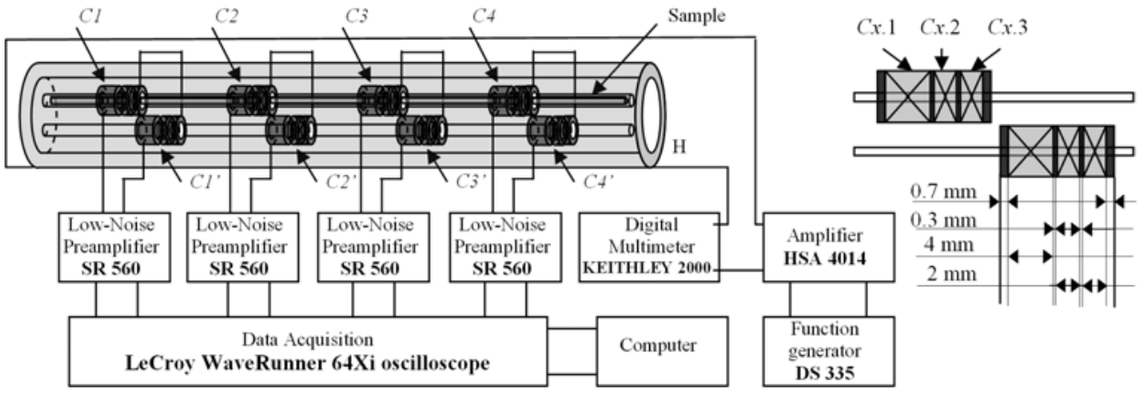

Fig. 6. Schematic of the system of four pairs of compensated pick-up coils.

Each pick-up coil is composed of three windings: a 4 mm long one with 1800 turns (*Cx*.1) and two 2 mm long ones with 800 turns (*Cx*.2 and *Cx*.3) placed close to the first one on the right side, all of them wound with enameled 0.07 mm copper wire on a ceramic tube with the outer diameter of 1.8 mm and the inner one of 1 mm. *Cx*.1, *Cx*.2 and *Cx*.3 are connected in series in the given order, with *Cx*.2 being wound in the opposite direction as compared to *Cx*.1 and *Cx*.3 in order to create a clear separation between the peaks induced in *Cx*.1 and

Cx.3. In order to reduce the self-oscillation of the system, an appropriate kilo-ohm resistor has been connected in parallel with each winding (4 kΩ for *Cx*.1 and 2 kΩ for *Cx*.2 and *Cx*.3, respectively). The pick-up coils are placed at certain distances among them (1 to 4 cm – depending on the wire characteristics).

There have been four pick-up coils used to measure the domain wall velocity in order to detect if any additional domain walls are nucleated in the measuring space and to obtain this way an accurate value of the wall velocity and not just an apparent one. The compensated system of pick-up coils can be employed to measure the wall velocity for bistable wires with diameters from tens of micrometers down to 100 nanometers (the smallest wire diameter tested) and for large values of the magnetizing field. For small wire diameters (below a few μm) the signals from the pick-up coils were amplified up to 50,000 times using four Stanford Research Systems SR560 low noise preamplifiers in order to obtain a measurable value of the induced voltage and a good signal to noise ratio.

The amplified signals were digitized using a four-channel LeCroy WaveRunner 64Xi oscilloscope, each of the four pick-up coils being connected to an input channel of the oscilloscope (*Cx* to input *Ix* , where x = 1, 2, 3, 4). An external trigger has been used in order to synchronize the acquired sample signal with the driving field. The current passing through the magnetizing solenoid (sinusoidal with a frequency of 160 Hz) was measured using a Keithley 2000 multimeter.

The acquired signals were processed using LabVIEW based software.

The inductive method is the most employed and straightforward technique used to measure the domain wall velocity in bistable microwires (Chiriac et al., 2009b; Garcia-Miquel et al., 2000; Ipatov et al., 2009). Various measuring configurations with two, three or four measuring points on the wire length were previously reported, each of them being a step forward for an enhanced and more precise measurement of the domain wall velocity in this type of wires.

The system with only two pick-up coils is not the most adequate for wall velocity measurements, since in the case of the wire, additional domain walls can nucleate at both ends of the wire and even at different points on the wire length when the driving field is large enough. Therefore, the signal picked up from one of the two coils is not precisely determined to be the result of the same domain wall as the signal picked up by the other coil. An apparent higher velocity than the real one can be recorded in this case.

Other measuring systems consist of four pick-up coils distributed on the wire length at a certain distance among them (Chiriac et al., 2008). This configuration provides information about the direction of the propagating wall. It also allows one to measure three values of the wall velocity and, if all of them are equal, then it is clear that there is a single wall propagating within the wire and the recorded wall velocity is the real one and not an apparent one. The main disadvantage of such a system is the impossibility to exactly identify the direction of the domain wall displacement through each coil.

This shortcoming has been solved by a recently proposed configuration which includes four pairs of pick-up coils which allow one to identify the direction of the wall propagation when it passes through each pair (Chiriac et al., 2009b). The main disadvantages of this set-up appear when the velocity is measured at large values of the applied field and/or when the measured wire has such a small diameter that the sample induced signal is much smaller

than the signal induced by the external field. In these cases, it is practically impossible to distinguish the sample-generated peaks in the recorded signal.

To overcome this matter, the following solution has been developed: two identical strips with four pairs of pick-up coils have been made according to the description given in (Chiriac et al., 2009b), with 2000 turns for the large coil and 800 turns for the smaller one, in order to increase the sensitivity. Each pair of coils from the first strip has been connected in series-opposition with a pair of coils from the second strip in order to cancel the signal induced by the applied field. The recorded signal had two peaks. However, this solution cannot be employed in the case of the ultrathin wires such as submicron wires and nanowires, because in this case the increment of the number of turns for each coil (made to increase sensitivity) leads to the impossibility to separate the two peaks. To overcome this new problem and to detect the direction of the domain wall displacement through the pick-up coil system, the measuring system has been improved with pick-up coils having three windings.

Figure 7 shows the compensated signals from each winding ($V_{Cx.1}$, $V_{Cx.2}$, $V_{Cx.3}$ – Figs. 7 a, b, c), the composed signal for all three windings $V_{Cx.1+2+3}=(V_{Cx.1})+(V_{Cx.2})+(V_{Cx.3})$, (Fig. 7 d), and the composed signal for the two windings wound in the same direction $V_{Cx.1+3}=(V_{Cx.1})+(V_{Cx.3})$, (Fig. 7 e), as they result from the separately acquired signals (x = 1, 2, 3, 4 – the number of the composite pick-up coil) for an $Fe_{77.5}Si_{7.5}B_{15}$ glass-coated microwire with the metallic nucleus diameter of 30 μm and the glass coating thickness of 25 μm. Signals have been acquired for two amplitudes of the applied field: 2 kA/m and 20 kA/m. The largest signal is given by *Cx*.1 and therefore its maximum is used as the marker for velocity calculations. The signal given by *Cx*.3 is smaller and is used to determine the direction of the wall movement in the pick-up coil system. For small values of the applied field and small

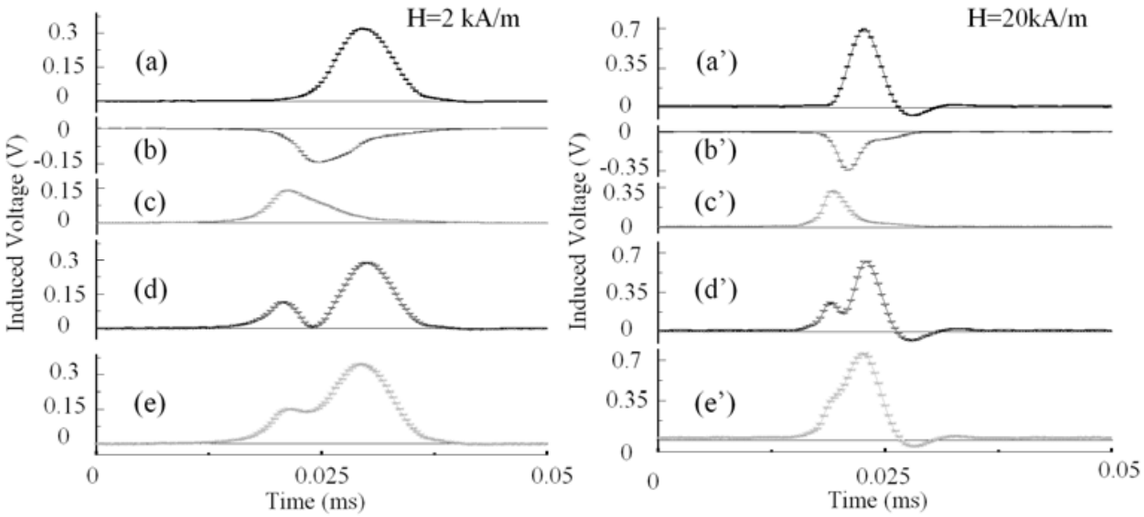

Fig. 7. Signals induced in each winding of a pick-up coil and in the pick-up coils composed of two and three windings for an $Fe_{77.5}Si_{7.5}B_{15}$ glass-coated microwire with the metallic nucleus diameter of 30 μm and the glass coating of 25 μm for two values of the applied field amplitude (2 kA/m and 20 kA/m): a, a') signal in C*x*.1; b, b') signal in C*x*.2; c, c') signal in C*x*.3; d, d') signal in the pick-up coil made of three windings; e, e') signal in the pick-up coil with two windings.

wall velocity values the system with pairs of two windings is enough to accurately detect the direction of the wall movement (Fig. 7 e).

The difficulties appear when the applied field and wall velocity increase and a net distinction between the positive peaks is no longer possible (Fig. 7 e'). By adding a new winding (*Cx*.2) in series-opposition with *Cx*.1 and *Cx*.3 (physically placed between these two) a net difference between the positive peaks appears, and the direction of wall displacement can be accurately determined even for larger applied fields and a corresponding wider range of wall velocity values.

The functionality of the system with pick-up coils composed of three windings has been tested on $Fe_{77.5}Si_{7.5}B_{15}$ amorphous glass-coated wires with metallic nucleus diameters from 30 μm down to 100 nm. The amplitude of the applied field was ranging between a few A/m and 2.5 kA/m. For small values of the metallic core diameter (below 1-2 μm) four low noise preamplifiers (Stanford Research Systems SR560) have been used in order to obtain a measurable voltage from each compound pick-up coil.

Figure 8 shows the peaks generated by the displacement of the domain wall in the sequence $C4 \rightarrow C3 \rightarrow C2 \rightarrow C1$, for an $Fe_{77.5}Si_{7.5}B_{15}$ glass-coated submicron amorphous wire with the metallic nucleus diameter of 500 nm and the glass coating thickness of 6.5 μm. The direction of the domain wall movement through each coil is determined from the order of the high and low amplitude peaks. The direction is from left to right ($C1 \rightarrow C2 \rightarrow C3 \rightarrow C4$) when the high amplitude peak appears ahead of the low amplitude one, and from right to left ($C4 \rightarrow C3 \rightarrow C2 \rightarrow C1$) when the high amplitude peak appears after the low amplitude one (see figures 7 and 8). Taking into account the succession of the amplitude peaks, one can observe that a single domain wall is propagating through the wire from right to left and the recorded wall velocity is therefore valid in this case, being 935 m/s at 3650 A/m for the tested submicron wire sample.

The distance between two neighboring pick-up coils was 40 mm. In some cases supplementary domain walls can be nucleated in the measuring space (Garcia-Miquel et al., 2000; Hudak et al., 2009), usually when a large field is applied and/or some defects are present in the wire structure. Therefore, for very high amplitudes of the applied field, the distance between two adjacent pick-up coils is reduced in order to measure the wall velocity, sometimes even down to 10 mm. This flexibility allows one to have a single domain wall moving through the measuring space for very high fields and for any sample diameter from 50 μm down to 300 nm.

However, for wires with the metallic nucleus diameter of 300 nm (see figure 9) and below, it is extremely difficult to discern the secondary peak (the smaller one) from the noise, since the amplitude of this peak is at the same level as the noise. Even so, measurements can be performed and the velocity of the domain wall is valid if the peaks are in the right order and all three measured values are equal. For the thinnest wire tested – the amorphous nanowire with the metallic nucleus diameter of 100 nm – the measurement of the wall velocity is even more difficult, as it displays a very large switching field (of about 11 kA/m), domain wall velocities above 1 km/s, and the distance which ensures that only propagation of a single domain wall takes place is very small, i.e. less than 3 cm.

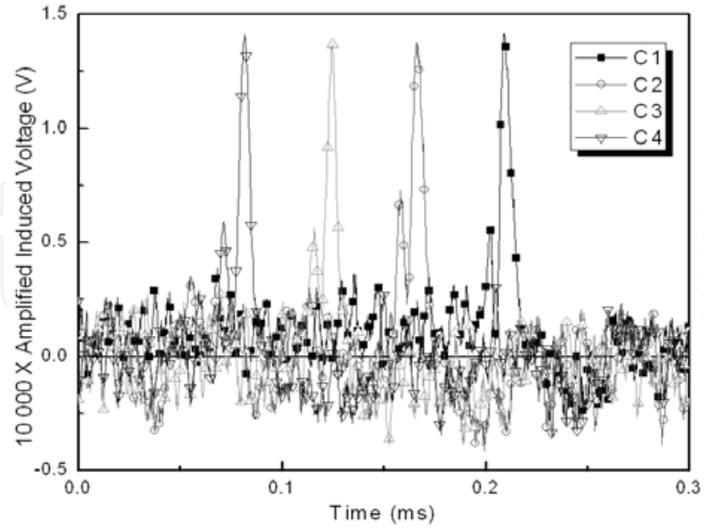

Fig. 8. Signal induced by the propagating wall in the sequence *C*4 → *C*3 → *C*2 → *C*1 in an $Fe_{77.5}Si_{7.5}B_{15}$ submicron amorphous wire with the metallic nucleus diameter of 500 nm. Applied field: 3,650 A/m.

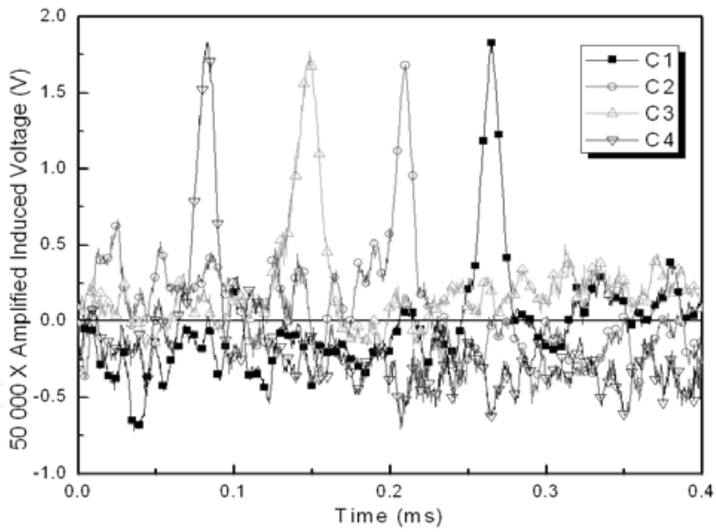

Fig. 9. Signal induced by the propagating wall in the sequence *C*4 → *C*3 → *C*2 → *C*1 in an $Fe_{77.5}Si_{7.5}B_{15}$ submicron amorphous wire with the metallic nucleus diameter of 300 nm and 6.5 μm glass thickness at 7,200 A/m.

Under these circumstances, the use of pick-up coils composed of three windings is no longer efficient. As a result, for wires with nucleus diameters below 300 nm, which display shorter propagation distances for the single wall, another specific system has been developed. The new specific system has four compensated 6 mm long pick-up coils with 1500 turns placed at 0.5 mm next to each other one, and wound with enameled 0.07 mm copper wire on a

ceramic tube with an outer diameter of 1.8 mm and the inner diameter of 1 mm. The distance between two adjacent coil centers (6.5 mm) and the time interval between the two corresponding peaks has been used to calculate the domain wall velocity. The resulting peaks and schematic view of the pick-up coil system are presented in figure 10.

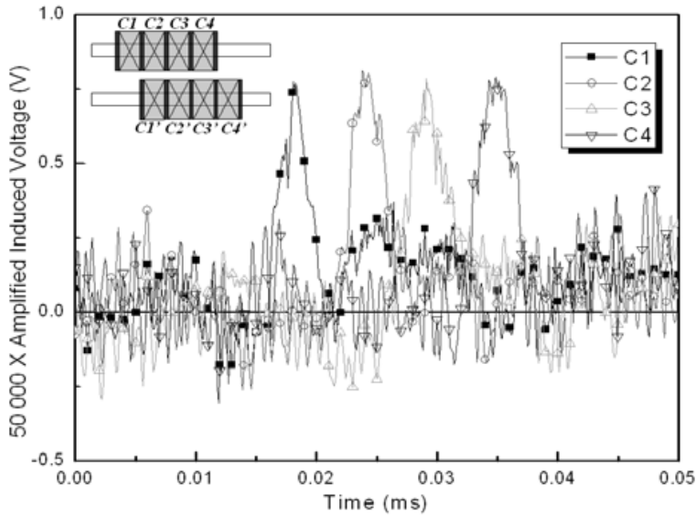

Fig. 10. Specific system of pick-up coils and signal induced by the wall in the sequence $C1 \rightarrow C2 \rightarrow C3 \rightarrow C4$ for an $Fe_{77.5}Si_{7.5}B_{15}$ nanowire with 100 nm nucleus diameter and 6 μm glass coating. Applied field: 1.5 kA/m.

Precision of the measured value of the wall velocity in this case is also ensured by the right order of the recorded peaks ($C1 \rightarrow C2 \rightarrow C3 \rightarrow C4$) and by the close values of all three recorded velocities ($V1$ = 1182 m/s, $V2$ = 1226 m/s, and $V3$ = 1140 m/s => $V \approx$ 1182 m/s). In the case of ultrathin wires some variations of the recorded velocity values always appear mainly due to the very low signal to noise ratio. The position of the maximum point in the peak, used for velocity calculation, is strongly affected by the noise.

A LabView application has been developed in order to reduce the measuring time and obtain a large number of points on the domain wall velocity versus field curves. A window, in which positive peaks are detected, is created and a zoom on this window is made to have all four peaks in view, in order to have always a visual control of the shape and order of the peaks. The software detects the position of the highest point from each trace and calculates three velocity values corresponding to the domain wall passing from $C1$ to $C2$, from $C2$ to $C3$, and from $C3$ to $C4$, respectively. The software records the velocities and relative peak positions and returns error messages if the succession of the peaks is not correct ($C1 \rightarrow C2 \rightarrow C3 \rightarrow C4$ or $C4 \rightarrow C3 \rightarrow C2 \rightarrow C1$) and if the recorded velocities differ by more than a certain predefined percent.

Figure 11 illustrates a comparative plot of the domain wall velocity vs. applied field for $Fe_{77.5}Si_{7.5}B_{15}$ amorphous microwires, submicron wires and nanowires, i.e. wires with different diameters of the metallic nucleus from the thickest (microwires with a 30 μm metallic nucleus) down to the thinnest (100 nm nanowires). The observed non-monotonic dependence of domain wall velocity on wire diameter is in agreement with previously

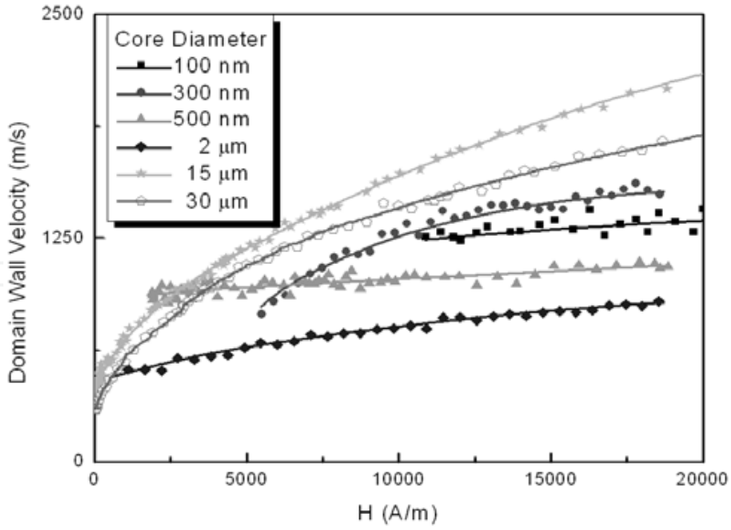

Fig. 11. Domain wall velocity in $Fe_{77.5}Si_{7.5}B_{15}$ amorphous glass-coated wires having various diameters of the metallic nucleus (microwires, submicron wires, and nanowires).

reported result for submicron amorphous wires (Óvári et al, 2011). Such comprehensive result would not have been possible without the development of the wall velocity measuring set-ups presented above.

The development of this new method was mainly requested by the inaccuracy of the current wall velocity measuring methods when the investigated samples are extremely thin, e.g. nanowires, which require very large fields to propagate a domain wall, fields which can nucleate additional domain walls and thus result in incorrect wall velocity values. Another reason which required the development of the novel method was the increment in sensitivity in order to measure domain wall velocity in wires with diameters down to 100 nm, in which the signal to noise ratio is very small. The proposed system is able to measure domain wall velocities between 50 and 2400 m/s for samples in which the magnetic flux is as low as 1.27×10^{-14} Wb. The availability of this new method is timely and of great importance at present, when much work is undertaken in order to develop novel domain wall logic devices which employ magnetic nanowires.

3. Magnetic behavior of rapidly solidified amorphous nanowires and submicron wires

3.1 800 nm submicron wires

The bulk and surface magnetic behavior of submicron amorphous wires have been investigated in order to compare them to the well known magnetic behavior of amorphous microwires and to monitor the changes induced as the threshold toward submicron dimensions is crossed.

The bulk magnetic behavior of the submicron wires has been studied by means of inductive hysteresis loops, obtained using a fluxmetric method. Due to the small value of the induced voltage in case of submicron wires, the signal was amplified using a Stanford Research Systems SR560 low-noise voltage preamplifier, and subsequently fed into the integrating fluxmeter.

The surface magnetic behavior has been investigated by magneto-optical Kerr effect (MOKE) in longitudinal configuration, using a NanoMOKE II magnetometer, produced by Durham Magneto Optics Ltd. In this case, the rotation of the plane of polarization was proportional to the magnetization component parallel to the plane of incidence. A polarized light of He-Ne laser (λ = 635 nm) was reflected from the wire to the detector. The diameter of the light beam was 2 μm and the penetration depth of the laser light is 9 nm. The plane of incidence was parallel to the wire axis. The following surface MOKE hysteresis loops have been measured: axial magnetization (M_Z) vs. axial field (H_Z), M_Z vs. perpendicular field ($H_\perp$), and M_Z vs. helical field ($H_{\theta Z}$).

Ferromagnetic resonance (FMR) measurements have been performed in order to study the magnetic anisotropy from the surface region of submicron wires and to correlate the results with the MOKE results. The FMR spectra were determined with an X-band spectrometer using the modulation technique. The DC magnetic field was modulated with an alternating field having a frequency of 1 kHz and the amplitude of 10 Oe. The working frequencies were 8.5, 9.5, and 10.5 GHz, respectively.

Figure 12 shows the axial inductive hysteresis loop of a submicron wire measured at 50 Hz. One observes that the submicron amorphous wire displays an unusual magnetic behavior, unlike microwires with the same composition and metallic nucleus diameters below 20 μm, which typically display an almost anhysteretic axial loop (Zhukov et al., 2003).

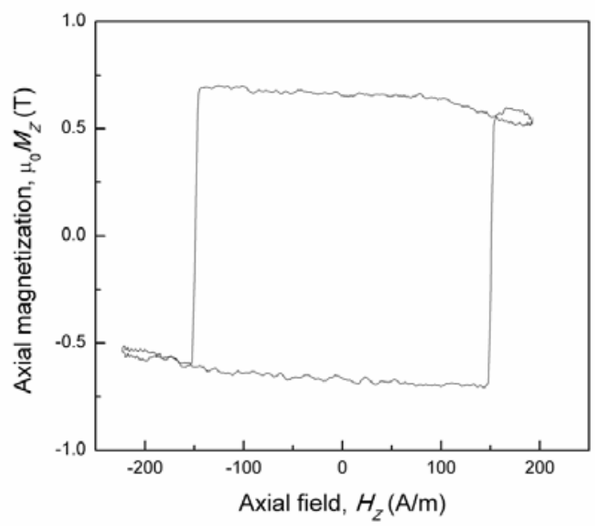

Fig. 12. Axial inductive hysteresis loop of a $(Co_{0.94}Fe_{0.06})_{72.5}Si_{12.5}B_{15}$ submicron amorphous glass-coated wire with the metallic nucleus diameter of 800 nm and the glass coating thickness of 6 μm.

On the contrary, the submicron wire is bistable even at such small diameter of the metallic nucleus, which shows shape anisotropy becomes more important than magnetoelastic anisotropy, which is prevailing in microwires with larger metallic nucleus diameters (several microns up to 20 μm). The value of the axial bulk switching field is 149 A/m, which is quite small for such low dimension.

Figure 13 illustrates the M_Z vs. H_Z MOKE surface hysteresis loop of the submicron amorphous wire. One observes that axial bistability is maintained even in the 9 nm deep

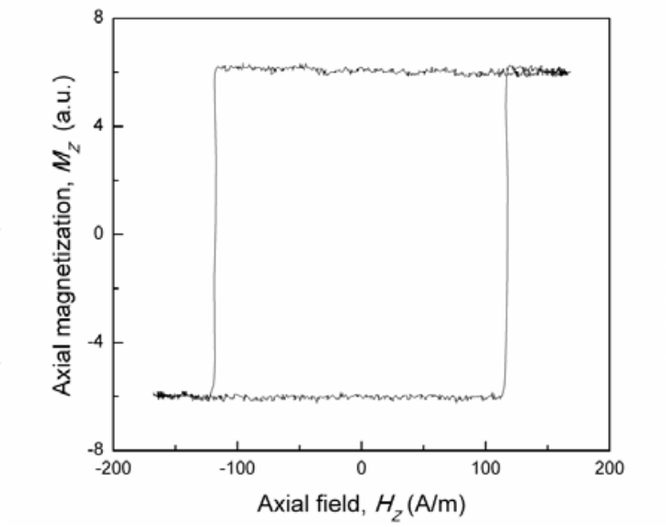

Fig. 13. Axial magnetization vs. axial field MOKE hysteresis loop for the $(Co_{0.94}Fe_{0.06})_{72.5}Si_{12.5}B_{15}$ submicron amorphous glass-coated wire.

surface region, and the surface axial switching field of 118 A/m is in the same range as the bulk value. This behavior is quite surprising, given the expected large values of the circumferential compressive stresses induced in the surface region during the preparation of the submicron wire. Nevertheless, it supports the above statement about the increased importance of shape anisotropy, and it shows that the submicron wire displays an axial component of magnetization in the surface region, as opposed to regular microwires with similar composition in which the outer shell is mostly circumferential.

Figure 14 shows the M_Z vs. $H_\perp$ MOKE surface loop of the submicron wire. The jump in magnetization is still observed, however the perpendicular switching field of 1600 A/m is one order of magnitude larger than the bulk axial switching field. This was expected, as $H_\perp$ does not act on the axial component of the magnetization M_Z, but only locally on the circumferential component M_θ, so a quite large field is required to switch the resultant surface magnetization $\boldsymbol{M}$ by acting only locally on one of its components, i.e. M_θ. The result of magnetization switching is monitored through the other component – M_Z.

Figure 15 illustrates the M_Z vs. $H_{\theta Z}$ MOKE surface loop for the same submicron amorphous wire. The magnetization jump is observed at a smaller value of the helical switching field, of 89 A/m. Results from figures 13 through 15 support the existence of helical magnetic anisotropy in the surface region of the submicron wire, rather than either solely axial or circumferential anisotropy. The small value of the helical switching field confirms the competition between magnetoelastic anisotropy and shape anisotropy and indicates a smaller overall anisotropy toward the surface, which is also in agreement with the decrease of the surface axial switching field (118 A/m) as compared to the value of the bulk axial switching field (149 A/m).

FMR has been employed to further investigate the surface anisotropy of the submicron amorphous wire. The values of the FMR line width at various frequencies for the submicron amorphous wire are listed in Table 1.

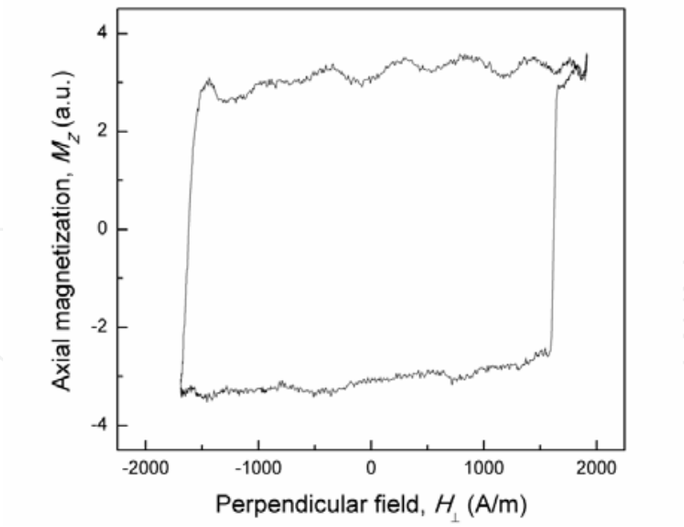

Fig. 14. Axial magnetization vs. perpendicular field MOKE hysteresis loop for the $(Co_{0.94}Fe_{0.06})_{72.5}Si_{12.5}B_{15}$ submicron amorphous glass-coated wire.

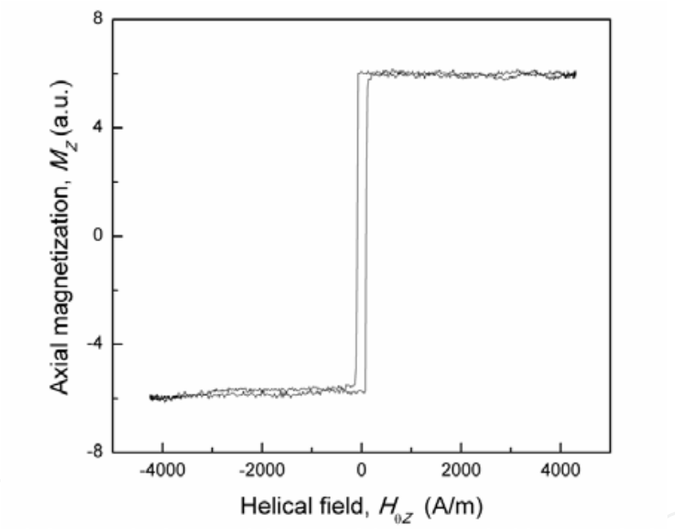

Fig. 15. Axial magnetization vs. helical field MOKE hysteresis loop for the $(Co_{0.94}Fe_{0.06})_{72.5}Si_{12.5}B_{15}$ submicron amorphous glass-coated wire.

Frequency (GHz)	Line width (kA/m) Submicron wire	Line width (kA/m) 6.5 μm microwire
8.5	5.65	11.94
9.5	6.29	13.53
10.5	6.37	14.57

Table 1. FMR line width values at various frequencies for the $(Co_{0.94}Fe_{0.06})_{72.5}Si_{12.5}B_{15}$ submicron amorphous glass-coated wire and for a microwire with the same composition having a 6.5 μm nucleus diameter and a 9.5 μm glass coating thickness.

The FMR line width at 8.5 GHz is less than half the value for a microwire with a 6.5 μm nucleus diameter, given for comparison. This shows that surface anisotropy is better emphasized in submicron wires as compared to microwires with typical dimensions, in agreement with larger stresses induced during preparation of these thinner samples. An increase of the resonance frequency to 9.5 and further to 10.5 GHz results in the increase of the line width, which shows a higher degree of anisotropy spread toward the surface and supports the above mentioned smaller overall anisotropy in the surface region.

Thus, the well known magnetic behavior of a typical nearly zero magnetostrictive microwire changes when the metallic nucleus diameter enters the submicron range. Shape anisotropy becomes dominant. Nearly zero magnetostrictive submicron wires are fully bistable, bistability being maintained even in a very thin 9 nm surface layer.

3.2 Submicron wires with diameters between 350 and 800 nm

A more significant effect of the reduction in the metallic nucleus diameter on the magnetic behavior of rapidly solidified $(Co_{0.94}Fe_{0.06})_{72.5}Si_{12.5}B_{15}$ nearly zero magnetostrictive and $Fe_{77.5}Si_{7.5}B_{15}$ positive magnetostrictive submicron wires has been investigated in a comparative manner. The investigated submicron wire samples display metallic nucleus diameters ranging from 350 to 800 nm. Their overall axial magnetization process has been studied by measuring the bulk inductive hysteresis loops using a fluxmetric method. A special attention has been also paid to the surface magnetic behavior of these thinner samples, which has been studied by means of MOKE and FMR.

Figure 16 shows the bulk axial hysteresis loops of a $(Co_{0.94}Fe_{0.06})_{72.5}Si_{12.5}B_{15}$ sample and an $Fe_{77.5}Si_{7.5}B_{15}$ sample with close values of the metallic nucleus diameter. The nearly zero magnetostrictive wire has a metallic nucleus diameter of 510 nm and the glass coating of 6.5 μm, whilst the positive magnetostrictive sample has the metallic nucleus diameter of 530 nm and a glass coating of 9.7 μm.

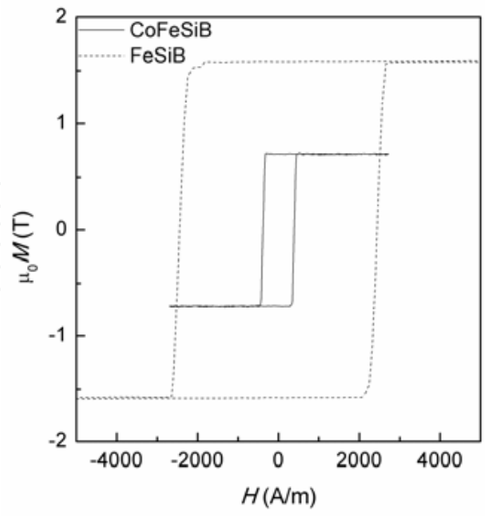

Fig. 16. Axial inductive hysteresis loops for a $(Co_{0.94}Fe_{0.06})_{72.5}Si_{12.5}B_{15}$ submicron amorphous wire with the metallic nucleus diameter of 510 nm and the glass coating of 6.5 μm and for an $Fe_{77.5}Si_{7.5}B_{15}$ sample with the metallic nucleus diameter of 530 nm and the glass coating of 9.7 μm.

The most important observation is that both types of submicron wires are indeed bistable, as proven by their rectangular hysteresis loops, which makes them suitable for spintronic applications. As concerns the particular aspects of these rectangular loops, besides the known differences in their saturation magnetization, one also observes the large difference between the coercivity values. The Co-based nearly zero magnetostrictive sample displays a coercivity of 350 A/m, whilst the Fe-based positive magnetostrictive submicron wire has a much larger coercivity of 2450 A/m. The correlation between dimensions, internal stresses and coercivity has been extensively studied in the case of the larger amorphous glass-coated microwires (Chiriac & Óvári, 1996). Such considerations also apply to the submicron wires, which are similarly composite wires prepared using the same technique. Therefore, coercivity is expected to decreases if the metallic nucleus diameter increases and/or the glass coating thickness decreases. Indeed, for a positive magnetostrictive submicron wire with the nucleus diameter of 670 nm and the glass coating of 6.5 μm, coercivity reaches down to 2000 A/m. This value shows that the coercivity of positive magnetostrictive submicron wires is strongly influenced by the magnetoelastic coupling between internal stresses and magnetostriction. However, the differences between the coercivity values in Fig. 16 cannot be entirely attributed to the different strength of the magnetoelastic coupling in positive and nearly zero magnetostrictive samples. A contribution is also given by the different nature of the uniaxial anisotropy: magnetoelastic in case of the positive magnetostrictive sample and shape anisotropy for the nearly zero magnetostrictive wire.

Coercivity increases to 4235 A/m for the thinnest positive magnetostrictive submicron wire (nucleus of 350 nm and coating of 6.5 μm). This is an expected consequence of the reduction in the metallic nucleus diameter, but it is difficult to estimate the role of shape anisotropy in this case.

Figure 17 illustrates the MOKE surface axial hysteresis loop of the 350 nm $Fe_{77.5}Si_{7.5}B_{15}$ submicron wire. The coercivity of the surface loop has the same value as the coercivity of the bulk loop. In case of the 510 nm nearly zero magnetostrictive submicron wire, the MOKE surface loop also shows the same coercivity value as the bulk one. These results show that the analyzed samples are bistable in their entire volume.

However, there is no information on whether or not the anisotropy is perfectly uniaxial in the near-surface region. FMR has been employed in order to study this particular aspect of the anisotropy distribution.

Figure 18 shows the FMR spectra of the $Fe_{77.5}Si_{7.5}B_{15}$ submicron amorphous wire with a metallic nucleus diameter of 350 nm. One observes that, irrespective of frequency, the derivative resonance spectra display a single resonance field. These results indicate that in such ultrathin submicron wires one can expect a uniaxial anisotropy which may show the presence of a single domain structure instead of the well known core-shell magnetic structure found in microwires (Chiriac & Óvári, 1996).

For comparison, figure 19 shows the FMR spectra of a typical $Fe_{77.5}Si_{7.5}B_{15}$ amorphous microwire with the metallic nucleus diameter of 22 μm and the glass coating thickness of 20 μm. One observes that the resonance peaks are split in this case, showing a complex anisotropy, which may be related to the typical outer shell and to the interdomain wall between the outer shell and the inner core encountered in microwires of this size (Chiriac et al., 2007b).

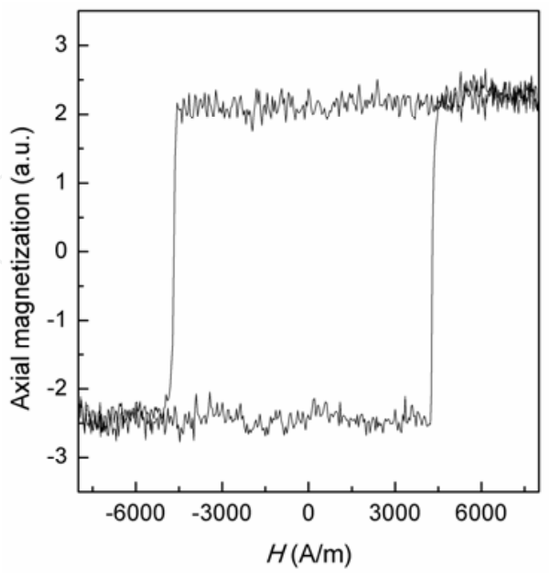

Fig. 17. MOKE surface axial hysteresis loop of an $Fe_{77.5}Si_{7.5}B_{15}$ submicron wire with the metallic nucleus diameter of 350 nm and the glass coating thickness of 6.5 μm.

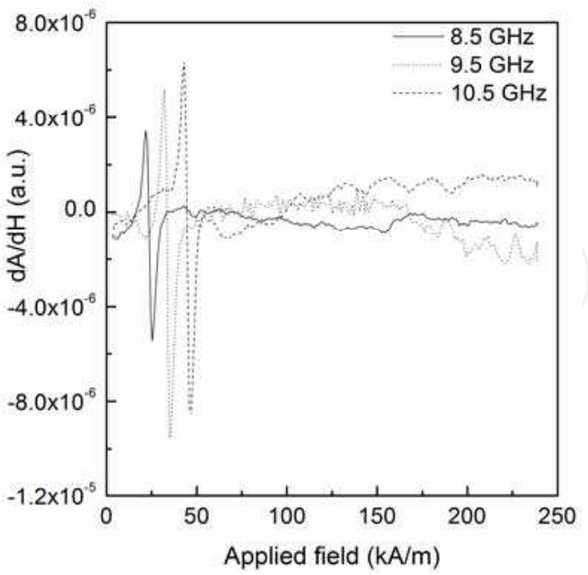

Fig. 18. FMR spectra of the $Fe_{77.5}Si_{7.5}B_{15}$ submicron amorphous wire with a metallic nucleus diameter of 350 nm and the glass coating thickness of 6.5 μm.

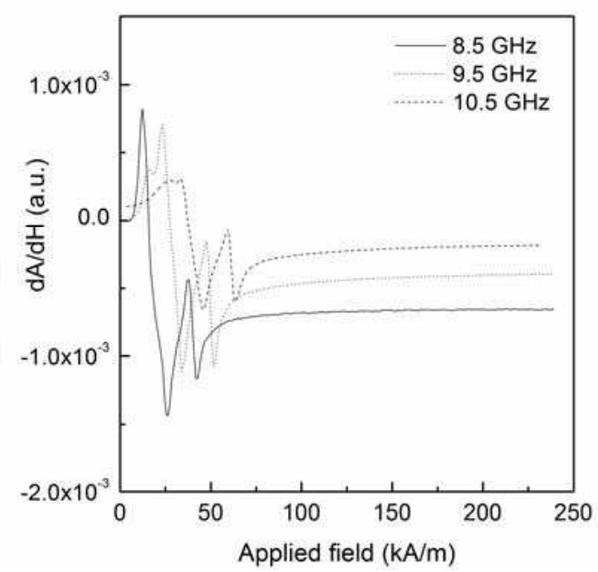

Fig. 19. FMR spectra of an $Fe_{77.5}Si_{7.5}B_{15}$ amorphous microwire with the metallic nucleus diameter of 22 μm and the glass coating thickness of 20 μm.

The most important result is that split resonance peaks have been found in this study even for $Fe_{77.5}Si_{7.5}B_{15}$ submicron wires with metallic nucleus diameters down to 500 nm. Figure 20 shows the FMR spectra of the $Fe_{77.5}Si_{7.5}B_{15}$ submicron wire with the metallic nucleus diameter of 530 nm and the glass coating thickness of 9.7 μm.

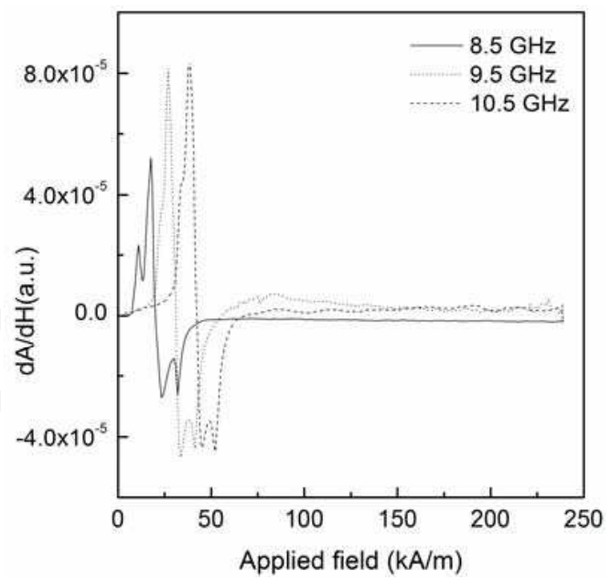

Fig. 20. FMR spectra of the $Fe_{77.5}Si_{7.5}B_{15}$ submicron wire with the metallic nucleus diameter of 530 nm and the glass coating thickness of 9.7 μm.

This shows that, even though the wire is fully bistable in its entire metallic nucleus, in the near-surface region there is a complex anisotropy which is different from the expected pure axial one. This is presumed to be a remnant of the radial anisotropy encountered in

amorphous microwires with the same composition (Chiriac & Óvári, 1996). It still produces effects which are detected by means of FMR due to the very large internal stresses produced by the existence of a large glass coating compared to the diameter of the metallic core. However, in the range from 500 nm to 350 nm an essential change occurs: shape anisotropy becomes much more important than the magnetoelastic one. Therefore, the 350 nm submicron wire is not only fully bistable, but it also displays a uniaxial anisotropy associated with the expected single domain magnetic structure.

In the case of nearly zero magnetostrictive submicron wires, the FMR spectra display only one maximum for nucleus diameters of either 800 nm or 500 nm. FMR does not emphasize the helical anisotropy observed by means of MOKE (Chiriac et al., 2010). This is an indication that the region with helical anisotropy is extremely thin, given that the penetration depth of the laser light is only 9 nm, and one can state that it is more a magnetization ripple located at the very surface of the metallic nucleus, rather than a well defined region with helical anisotropy. Such statement is in agreement with the axial magnetic bistability determined by shape anisotropy in the $(Co_{0.94}Fe_{0.06})_{72.5}Si_{12.5}B_{15}$ samples.

Thus, the crucial role played by shape anisotropy in the magnetic behavior of these ultrathin magnetic wires has been emphasized once more. Shape anisotropy is the main factor that determines the bistability of nearly zero magnetostrictive submicron wires, irrespective of the diameter of their metallic nucleus. This is due to their much smaller magnetoelastic term, which originates in their small negative magnetostriction. As a result, they display a single domain magnetic structure with an ultrathin magnetization ripple at the surface. On the other hand, in positive magnetostrictive samples, magnetoelastic anisotropy still plays an important role in wires with nucleus diameters from 500 nm and up, as shown by the FMR spectra. In thinner samples, shape anisotropy becomes dominant and therefore they display a single domain magnetic structure.

3.3 Rapidly solidified amorphous nanowires

Figure 21 shows the bulk hysteresis loops for two rapidly solidified glass-coated amorphous nanowire samples. One observes the significant difference between the two switching fields – 420 A/m as compared to 7400 A/m.

Figure 22 illustrates the MOKE surface hysteresis loop for the same samples. Both loops show that the nanowires are bistable in their entire volume. This is an indication that rapidly quenched amorphous magnetic nanowires display a single-domain structure, as opposed to the classical core-shell structure (Takajo et al., 1993; Vázquez, 2001) of the thicker amorphous microwires (metallic nucleus diameters over 1 μm) and of the submicron amorphous wires with diameters between 500 and 900 nm.

Therefore, at nanoscale, irrespective of composition, sample dimensions no longer allow the formation of a complex core-shell magnetic domain structure as a result of magnetoelastic energy minimization (Chiriac et al., 1995; Velázquez et al., 1996). Hence, despite the larger values of the internal stresses in these ultra-thin rapidly solidified materials, which coupled with the large positive magnetostriction of the $Fe_{77.5}Si_{7.5}B_{15}$ alloy lead to a large magnetoelastic term, the shape anisotropy is preponderant at nanoscale. The large internal stresses induced by both rapid solidification of metal and the difference between the thermal expansion coefficients of metal and glass (Chiriac et al., 1995) give rise to quite large values of the switching field, as shown in Figures 20 and 21.

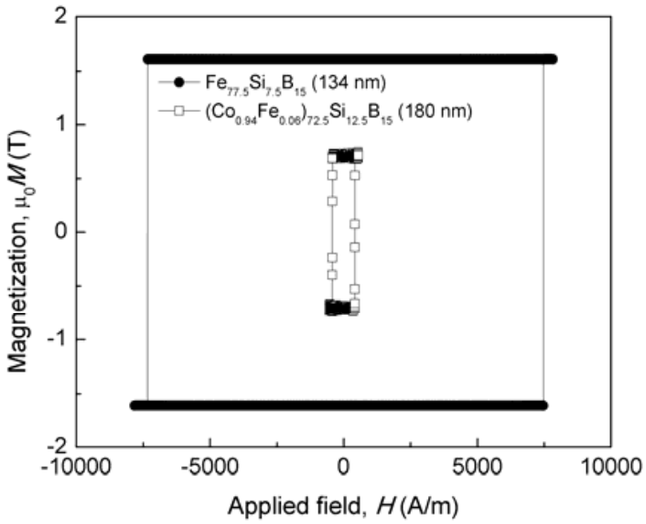

Fig. 21. Axial inductive hysteresis loops of two rapidly solidified amorphous nanowires: one with positive magnetostriction having the metallic nucleus diameter of 134 nm and the glass coating thickness of 6 μm and the other one with nearly zero magnetostriction having the metallic nucleus diameter of 180 nm and the glass coating thickness of 5.6 μm.

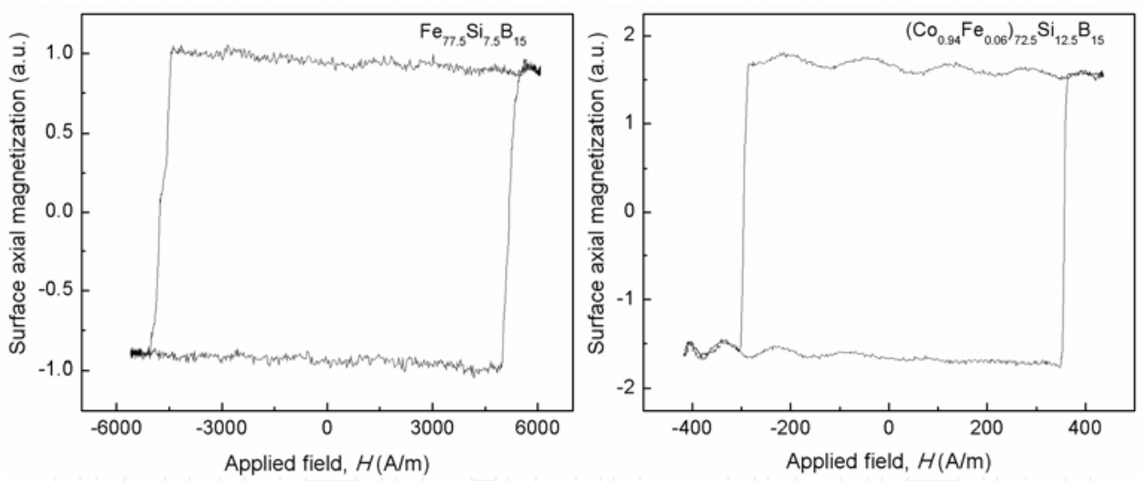

Fig. 22. Axial magnetization vs. axial field MOKE hysteresis loop for the rapidly solidified amorphous nanowire with positive magnetostriction (left) and for the one with nearly zero magnetostriction (right).

The direct relation between the value of the switching field and the glass to metal ratio is well known (Chiriac et al., 1997). In case of the $(Co_{0.94}Fe_{0.06})_{72.5}Si_{12.5}B_{15}$ samples magnetostriction is much smaller leading to smaller values of the switching field. Thus, there is a wide range of possibilities to adjust the value of the switching field by changing the composition or by partially or fully removing the glass coating. First glass removal experiments have been successful, with the glass coating being thinned down to 10 nm.

The difference between the values of the switching field for the bulk and surface loops originate in the surface defects of the metallic nucleus as well as in the demagnetizing effect,

which are expected to cause a slight magnetization ripple at the surface, i.e. small local deviations of the magnetization from the axial direction. Such deviations are more easily emphasized in MOKE measurements on nearly zero magnetostrictive samples, when the field is applied transversally to the nanowire.

In order to substantiate the existence of the single domain structure in the rapidly solidified glass-coated amorphous magnetic nanowires, further investigations by means of FMR have been performed on positive magnetostrictive nanowires. The aim was to investigate the effect of the large magnetoelastic term at the wire surface, where the outer shell should exist.

Figure 23 shows the derivative microwave absorption spectrum of the $Fe_{77.5}Si_{7.5}B_{15}$ amorphous nanowire (left). For comparison, the spectrum of a rapidly solidified 800 nm submicron amorphous wire with the same composition is given (right).

The FMR spectrum of the submicron wire displays split resonance peaks, which reflect a complex anisotropy, which may indicate the presence of the complex core-shell domain structure. On the other hand, the FMR spectrum of the rapidly solidified amorphous nanowire does not display such a split, showing a single anisotropy direction at all frequencies, which supports the existence of a single domain structure.

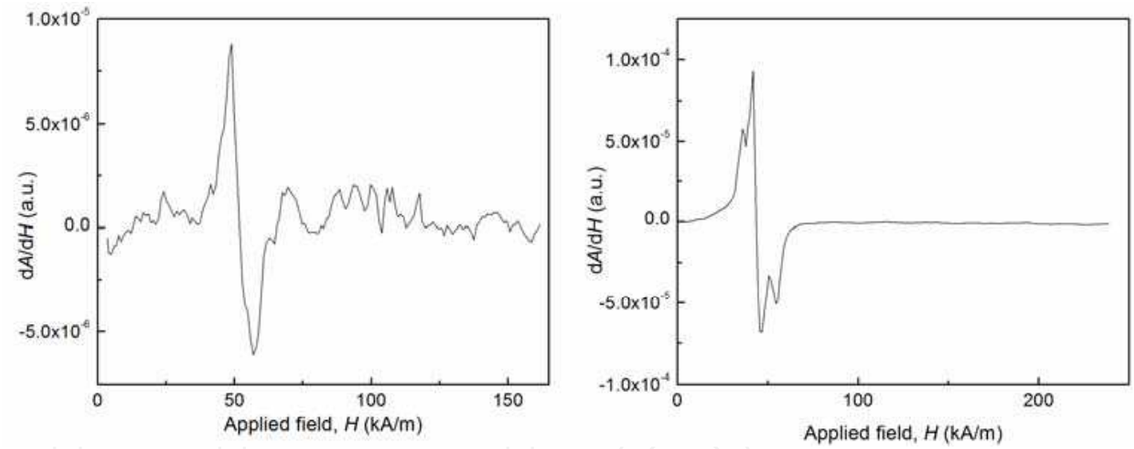

Fig. 23. Microwave absorption spectrum of the 134 nm $Fe_{77.5}Si_{7.5}B_{15}$ amorphous nanowire (left) and of an 800 nm $Fe_{77.5}Si_{7.5}B_{15}$ submicron amorphous wire (right) at 10.5 GHz.

Thus, both FMR and hysteresis loop measurements (inductive and MOKE) point to the existence of a single domain structure in rapidly solidified amorphous glass-coated nanowires. The large magnetoelastic term cannot exceed the shape anisotropy in positive magnetostrictive amorphous nanowires. This is even less likely to happen in the nearly zero magnetostrictive nanowires, given their much smaller magnetoelastic term.

The uniaxial magnetization in the whole volume of the amorphous nanowire is favored by shape anisotropy. This means that the nanowires are too thin to allow the formation of a more complex magnetic domain structure. Therefore, such nanowires are the perfect candidates for spintronic applications based on the domain wall propagation along the entire length of the sample.

4. Domain wall velocity in rapidly solidified amorphous nanowires and submicron wires

The study of the domain wall velocity in bistable submicron amorphous wires with positive and nearly zero magnetostriction prepared by rapid solidification from the melt is closely linked to the purpose for which submicron wires have been prepared, i.e. to understand the characteristics of domain wall propagation in the thinnest possible wires made by rapid solidification, in order to propose new materials for spintronic applications. The effect of wire dimensions on wall velocity is studied in conjunction with their magnetic behavior. The role of magnetostriction in these ultrathin wires is also analyzed. The employed experimental set-ups are those described in detail in section 2.2.

Figure 24 shows the dependence of wall velocity on applied field for $Fe_{77.5}Si_{7.5}B_{15}$ positive magnetostrictive amorphous submicron wires with different metallic nucleus diameters and the same glass coating thickness of 15 μm. Figure 25 illustrates the axial hysteresis loops for the same samples.

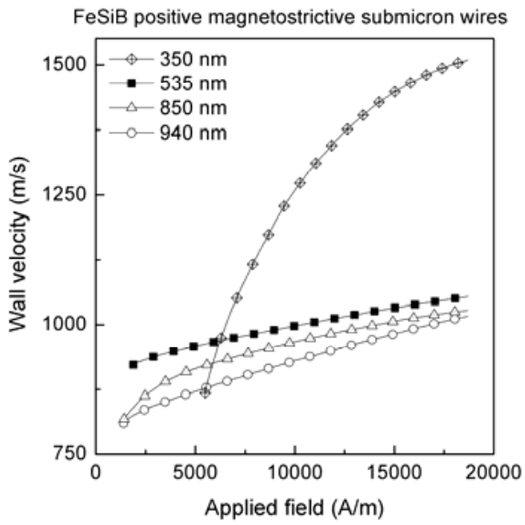

Fig. 24. Wall velocity vs. applied field for $Fe_{77.5}Si_{7.5}B_{15}$ submicron amorphous wires with positive magnetostriction, having different metallic nucleus diameters and a similar glass coating thickness (15 μm).

A correlation between the domain wall velocity and the value of the switching field is observed, i.e. the larger the switching field, the larger the wall velocity, which indicates a relation between the magnitude of the uniaxial anisotropy and the domain wall velocity. However, something is different for the sample with the 350 nm nucleus diameter: the slope of its wall velocity vs. applied field curve, i.e. the wall mobility, is significantly larger than the slope of the curves which correspond to the other samples. This shows that something is different about the uniaxial anisotropy of this sample. If in case of the thicker samples one would expect a closely related cause of the uniaxial anisotropy with the case of typical amorphous microwires, i.e. the magnetoelastic coupling between the large axial internal stresses and the positive magnetostriction, in case of the thinnest one, the role of magnetoelastic anisotropy is taken over by the shape anisotropy, as mentioned in the previous sections.

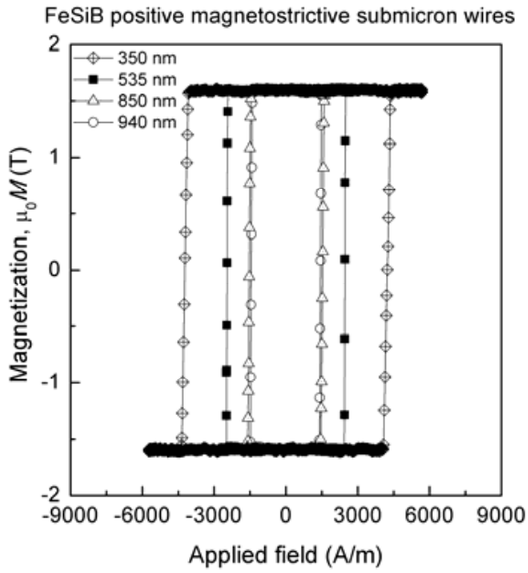

Fig. 25. Axial hysteresis loops for $Fe_{77.5}Si_{7.5}B_{15}$ submicron amorphous wires with positive magnetostriction, having different metallic nucleus diameters and a similar glass coating thickness (15 μm).

Thus, the effect of internal stresses is diminished as the metallic nucleus diameter decreases below a certain threshold, and the applied field becomes much more efficient in moving the domain wall, which results in increased mobility and velocity values. Therefore, the increased contribution of shape anisotropy results in larger wall velocity and mobility values in the case of positive magnetostrictive submicron wires.

The largest wall velocity value is close to 1500 m/s, close to the largest values reported in microwires with the same composition and with typical dimensions in the range 1-50 μm.

Figure 26 shows the dependence of wall velocity on applied field for two $(Co_{0.94}Fe_{0.06})_{72.5}Si_{12.5}B_{15}$ nearly zero magnetostrictive submicron wire samples with different metallic nucleus diameters and the same glass coating thickness of 13 μm. Figure 27 illustrates the corresponding axial hysteresis loops. The correlation between wall velocity and uniaxial anisotropy, via switching field, is also observed in the case of submicron wires with nearly zero magnetostriction. However, in this case only shape anisotropy contributes to larger wall velocity values, as opposed to the case of positive magnetostrictive microwires, in which magnetoelastic anisotropy also has some contribution, at least down to a certain threshold. Given the negative sign of magnetostriction in the nearly zero magnetostrictive samples, the magnetoelastic anisotropy would lead to transverse uniaxial anisotropy instead of an axial one. Therefore, it is clear that the magnetic bistability of these samples originates in an axial anisotropy determined by shape anisotropy only.

The maximum velocity values measured in nearly zero magnetostrictive submicron wires are slightly larger at about 1600 m/s than those measured in positive magnetostrictive ones. Nevertheless, these large velocities are obtained at much smaller values of the applied field in comparison with the case of positive magnetostrictive samples, i.e. 200 to 600 A/m as compared to 0.7 to 18 kA/m. Again, wall mobility is larger in thinner submicron wires, similar to the case of positive magnetostrictive samples, which substantiates the essential

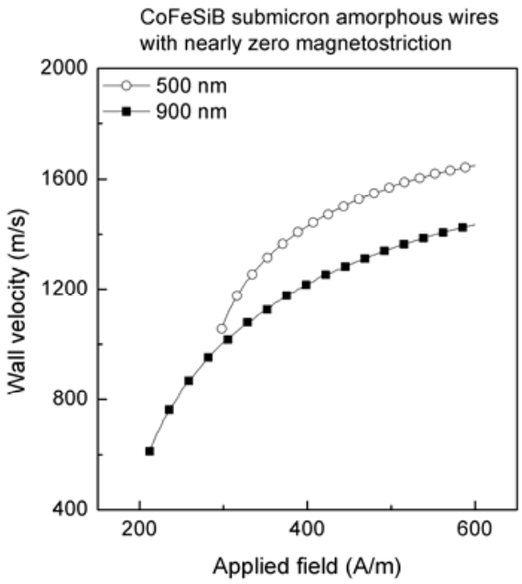

Fig. 26. Wall velocity vs. applied field for two $(Co_{0.94}Fe_{0.06})_{72.5}Si_{12.5}B_{15}$ submicron amorphous wires with nearly zero magnetostriction, having different metallic nucleus diameters and the same glass coating thickness (13 μm).

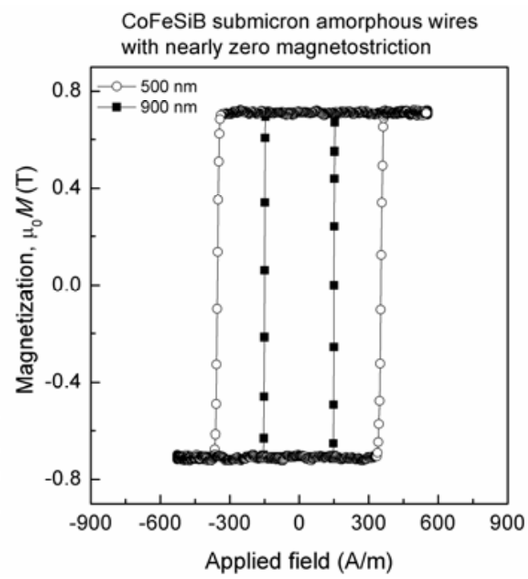

Fig. 27. Axial hysteresis loops for two $(Co_{0.94}Fe_{0.06})_{72.5}Si_{12.5}B_{15}$ submicron amorphous wires with nearly zero magnetostriction, having different metallic nucleus diameters and the same glass coating thickness (13 μm).

role played by shape anisotropy in both types of submicron wires. The wall velocity values are comparable to those measured in planar NiFe nanowires (Atkinson et al., 2003), although the mobility values are significantly larger in the case of nearly zero magnetostrictive submicron wires. Thus, both the wire dimensions and the magnetostriction are important as concerns the domain wall velocity and mobility values in rapidly solidified

amorphous submicron wires. Wire dimensions influence the shape anisotropy, whilst magnetostriction affects the magnetoelastic anisotropy. Both anisotropy types play an important role in submicron wires with positive magnetostriction. In negative magnetostrictive ones, only shape anisotropy plays an essential role.

Figure 28 illustrates the field dependence of the domain wall velocity in the 134 nm rapidly solidified nanowire with positive magnetostriction (left) and in the 180 nm one with nearly zero magnetostriction (right).

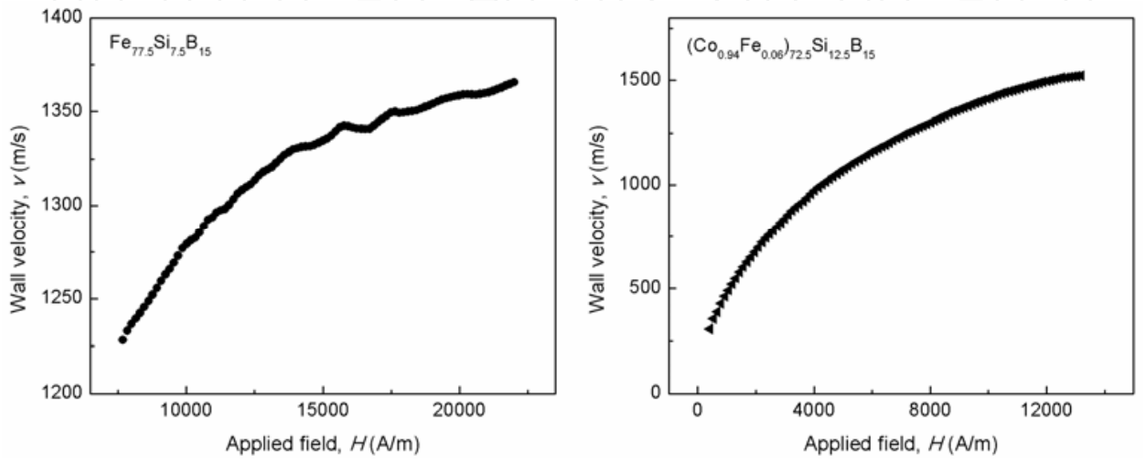

Fig. 28. Wall velocity vs. applied field for a rapidly solidified $Fe_{77.5}Si_{7.5}B_{15}$ amorphous nanowire with positive magnetostriction, having the metallic nucleus diameter of 134 nm and the glass coating thickness of 6 μm (left) and for a $(Co_{0.94}Fe_{0.06})_{72.5}Si_{12.5}B_{15}$ nearly zero magnetostrictive one with the metallic nucleus diameter of 180 nm and the glass coating thickness of 5.6 μm (right).

For the positive magnetostrictive sample the maximum wall velocity, reached at an applied field larger than 20 kA/m, is above 1360 m/s. Nevertheless, even at an applied field just above the value of the switching field the wall velocity is larger than 1200 m/s. These values are also comparable to those reported in planar NiFe nanowires (Atkinson et al., 2003) and they are expected to improve after glass removal. Although the mobility of the wall is rather small (velocity does not increase much with the applied field), this aspect is also expected to significantly improve after glass removal as a result of stress relief and decrease of the switching field. Wall velocity values are larger, over 1500 m/s, in the case of nearly zero magnetostrictive samples, and they are attained at much smaller values of the applied field. The wall mobility in these nanowires is also much larger. This shows the importance of composition for spintronic applications. These results are important as concerns the future application of rapidly solidified nanowires and submicron wires in spintronic devices.

5. Conclusions

Rapidly solidified magnetic nanowires and submicron wires have low production costs and their properties can be accurately tailored through a variety of parameters, known from

their larger precursors – the amorphous microwires: the diameter of the metallic nucleus, the glass coating thickness, their ratio, and the composition, which decides the sign and magnitude of the magnetostriction constant. These tailoring parameters are adjustable through the preparation process. Post-production processing, such as various types of annealing (furnace, Joule heating, field-annealing, stress-annealing) as well as the post-production partial or full removal of the glass coating can be also used to tailor the magnetic properties. Tailoring parameters facilitate the fine tuning of nanowire and submicron wire properties. Another advantage of the rapidly solidified amorphous nanowires and submicron wires is that they can be prepared at sample lengths which basically exceed all the current requirements of applications based on nanowire samples.

The preparation of these materials has been successful since it was initially based on well known materials, which have been extensively studied at the larger micro scale. We have been able to prepare them at a much smaller scale, the nano and submicron scale, aiming to preserve their specific characteristics and properties within certain limits.

Future work will focus on tailoring the wall propagation characteristics, such as velocity and mobility. The technical solutions used for the preparation of amorphous magnetic nanowires should be extended, to permit the preparation of a much larger range of compositions. Such development would lead to novel applications, e.g. medical, various sensors, controlled motion of particles. Magnetic nanowires are also suitable for shielding applications at very high frequencies.

6. Acknowledgment

Work supported by the Romanian Ministry of Education, Research, Youth and Sports through the NUCLEU Program (Contracts No. 09-43 N, 01 02, 02 04, and PN 09-43 01 01) and through the PARTENERIATE Program under Contract No. 82-096/2008 (NADEX).

7. References

Allwood, D.A.; Xiong, G.; Faulkner, C.C.; Atkinson, D.; Petit, D. & Cowburn, R.P. (2005). Magnetic Domain-Wall Logic. *Science,* Vol.309, No.5741, (September 2005), pp. 1688-1692, ISSN 0036-8075

Atkinson, D.; Allwood, D.A.; Faulkner, C.C.; Xiong, G.; Cooke, M.D. & Cowburn, R.P. (2003). Magnetic Domain Wall Dynamics in a Permalloy Nanowire. *IEEE Transactions on Magnetics,* Vol.39, No.5, (September 2003), pp. 2663-2665, ISSN 0018-9464

Butta, M.; Infante, G.; Ripka, P.; Badini-Confalonieri, G.A. & Vázquez, M. (2009). M-H Loop Tracer Based on Digital Signal Processing for Low Frequency Characterization of Extremely Thin Magnetic Wires. *Review of Scientific Instruments,* Vol.80, No.8, (August 2009), 083906, ISSN 0034-6748

Chiriac, H.; Óvári, T.-A. & Pop, G. (1995). Internal Stress Distribution in Glass-Covered Amorphous Magnetic Wires. *Physical Review B,* Vol.52, No.14, (October 1995), pp. 10104-10113, ISSN 1098-0121

Chiriac, H. & Óvári, T.-A. (1996). Amorphous Glass-Covered Magnetic Wires: Preparation, Properties, Applications. *Progress in Materials Science,* Vol.40, No.5, (December 1996), pp. 333-407, ISSN 0079-6425

Chiriac, H.; Óvári, T.-A.; Pop, G. & Bararіu, F. (1997). Effect of Glass Removal on the Magnetic Behavior of FeSiB Glass-Covered Wires. *IEEE Transactions on Magnetics,* Vol.33, No.1, (January 1997), pp. 782-787, ISSN 0018-9464

Chiriac, H.; Corodeanu, S.; Ţibu, M. & Óvári, T.-A. (2007a). Size Triggered Change in the Magnetization Mechanism of Nearly Zero Magnetostrictive Amorphous Glass-Coated Microwires. *Journal of Applied Physics,* Vol.101, No.9, (May 2007), 09N116, ISSN 0021-8979

Chiriac, H.; Óvári, T.-A.; Corodeanu, S. & Ababei, G. (2007b). Interdomain Wall in Amorphous Glass-Coated Microwires. *Physical Review B,* Vol.76, No.21, (December 2007), 214433, ISSN 1098-0121

Chiriac, H.; Óvári, T.-A. & Ţibu, M. (2008). Domain Wall Propagation in Nearly Zero Magnetostrictive Amorphous Microwires. *IEEE Transactions on Magnetics,* Vol.44, No.11, (November 2008), pp. 3931-3933, ISSN 0018-9464

Chiriac, H.; Óvári, T.-A. & Ţibu, M. (2009a). Effect of Surface Domain Structure on Wall Mobility in Amorphous Microwires. *Journal of Applied Physics,* Vol.105, No.7, (April 2009), 07A310, ISSN 0021-8979

Chiriac, H.; Ţibu, M. & Óvári, T.-A. (2009b). Domain Wall Propagation in Nanocrystalline Glass-Coated Microwires. *IEEE Transactions on Magnetics,* Vol.45, No.10, (October 2009), pp. 4286-4289, ISSN 0018-9464

Chiriac, H. ; Corodeanu, S. ; Lostun, M. ; Ababei, G. & Óvári, T.-A. (2010). Magnetic Behavior of Rapidly Quenched Submicron Amorphous Wires. *Journal of Applied Physics,* Vol.107, No.9, (May 2010), 09A301, ISSN 0021-8979

Chiriac, H.; Lostun, M.; Ababei, G.; & Óvári, T.-A. (2011a). Comparative Study of the Magnetic Properties of Positive and Nearly Zero Magnetostrictive Submicron Amorphous Wires. *Journal of Applied Physics,* Vol.109, No.7, (April 2011), 07B501, ISSN 0021-8979

Chiriac, H.; Corodeanu, S.; Lostun, M.; Stoian, G.; Ababei, G. & Óvári, T.-A. (2011b). Rapidly Solidified Amorphous Nanowires. *Journal of Applied Physics,* Vol.109, No.6, (March 2011), 063902, ISSN 0021-8979

Corodeanu, S.; Chiriac, H.; Lupu, N. & Óvári, T.-A. (2011a). Magnetic Characterization of Submicron Wires and Nanowires Using Digital Integration Techniques. *IEEE Transactions on Magnetics,* vol.47, No.10, (October 2011), pp. 3513-3515, ISSN 0018-9464

Corodeanu, S.; Chiriac, H. & Óvári, T.-A. (2011b). Accurate Measurement of Domain Wall Velocity in Amorphous Microwires, Submicron Wires, and Nanowires. *Review of Scientific Instruments,* Vol.82, No.9, (September 2011), 094701, ISSN 0034-6748

Finocchio, G.; Maugeri, N.; Torres, L. & Azzerboni, B. (2010). Domain Wall Dynamics Driven by a Localized Injection of a Spin-Polarized Current. *IEEE Transactions on Magnetics,* Vol.46, No.6, (June 2010), pp. 1523-1526, ISSN 0018-9464

Garcia-Miquel, H.; Chen, D.-X. & Vázquez, M. (2000). Domain Wall Propagation in Bistable Amorphous Wires. *Journal of Magnetism and Magnetic Materials,* Vol.212, Nos.1-2, (March 2000), pp. 101-106, ISSN 0304-8853

Hudak, J.; Blazek, J.; Cverha, A.; Gonda, P. & Varga, R. (2009). Improved Sixtus-Tonks Method for Sensing the Domain Wall Propagation Direction. *Sensors and Actuators A: Physical,* Vol.156, No.2, (December 2009), pp. 292-295, ISSN 0924-4247

Ipatov, M.; Zhukova, V.; Zvezdin, A.K. & Zhukov, A. (2009). Mechanisms of the Ultrafast Magnetization Switching in Bistable Amorphous Microwires. *Journal of Applied Physics,* Vol.106, No.10, (November 2009), 103902, ISSN 0021-8979

Komova, E.; Varga, M.; Varga, R.; Vojtanik, P.; Bednarcik, J.; Kovac, J.; Provencio, M. & Vázquez, M. (2008). Nanocrystalline Glass-Coated FeNiMoB Microwires. *Applied Physics Letters,* Vol.93, No.6, (August 2008), 062502, ISSN 0003-6951

Kulik, T.; Savage, H.T. & Hernando, A. (1993). A High-Performance Hysteresis Loop Tracer. *Journal of Applied Physics,* Vol.73, No.10, (May 1993), pp. 6855-6857, ISSN 0021-8979

Lee, J.Y.; Lee, K.S. & Lee, S.K. (2007). Remarkable Enhancement of Domain-Wall Velocity in Magnetic Nanostripes. *Applied Physics Letters,* Vol.91, No.12, (September 2007), 122513, ISSN 0003-6951

Moriya, R.; Hayashi, M.; Thomas, L.; Rettner, C. & Parkin, S.S.P. (2010). Dependence of Field Driven Domain Wall Velocity on Cross-Sectional Area in $Ni_{65}Fe_{20}Co_{15}$ Nanowires. *Applied Physics Letters,* Vol.97, No.14, (October 2010), 142506, ISSN 0003-6951

Óvári, T.-A.; Corodeanu, S. & Chiriac, H. (2011). Domain Wall Velocity in Submicron Amorphous Wires. *Journal of Applied Physics,* Vol.109, No.7, (April 2011), 07D502, ISSN 0021-8979

Parkin, S.S.P.; Hayashi, M. & Thomas, L. (2008). Magnetic Domain-Wall Racetrack Memory. *Science,* Vol.320, No.5873, (April 2008), pp. 190-194, ISSN 0036-8075

Sixtus, K.J. & Tonks, L. (1932). Propagation of Large Barkhausen Discontinuities. II. *Physical Review,* Vol.42, No.3, (November 1932), pp. 419-435

Takajo, M.; Yamasaki, J. & Humphrey, F.B. (1993). Domain Observations of Fe and Co Based Amorphous Wires. *IEEE Transactions on Magnetics,* Vol.29, No.6, (November 1993), pp. 3484-3486, ISSN 0018-9464

Torrejón, J.; Vázquez, M. & Panina, L.V. (2009). Asymmetric Magnetoimpedance in Self-Biased Layered CoFe/CoNi Microwires. *Journal of Applied Physics,* Vol.105, No.3, (February 2009), 033911, ISSN 0021-8979

Vázquez, M. (2001). Soft Magnetic Wires. *Physica B: Condensed Matter,* Vol.299, Nos.3-4, (June 2001), pp. 302-313, ISSN 0921-4526

Vázquez, M.; Basheed, G.A.; Infante, G. & Del Real, R.P. (2012). Trapping and Injecting Single Domain Walls in Magnetic Wire by Local Fields. *Physical Review Letters,* Vol.108, No.3, (January 2012), 037201, ISSN 0031-9007

Velázquez, J.; Vázquez, M. & Zhukov, A.P. (1996). Magnetoelastic Anisotropy Distribution in Glass-Coated Microwires. *Journal of Materials Research,* Vol.11, No.10, (October 1996), pp. 2499-2505, ISSN 0884-2914

Zhukov, A.; Zhukova, V.; Blanco, J.M.; Cobeño, A.F.; Vázquez, M. & González, J. (2003). Magnetostriction in Glass-Coated Magnetic Microwires. *Journal of Magnetism and Magnetic Materials,* Vols.258-259, (March 2003), pp. 151-157, ISSN 0304-8853

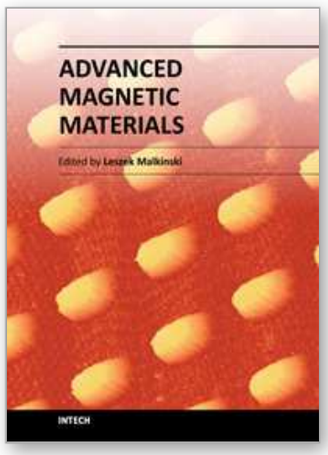

Advanced Magnetic Materials

Edited by Dr. Leszek Malkinski

ISBN 978-953-51-0637-1
Hard cover, 230 pages
Publisher InTech
Published online 24, May, 2012
Published in print edition May, 2012

This book reports on recent progress in emerging technologies, modern characterization methods, theory and applications of advanced magnetic materials. It covers broad spectrum of topics: technology and characterization of rapidly quenched nanowires for information technology; fabrication and properties of hexagonal ferrite films for microwave communication; surface reconstruction of magnetite for spintronics; synthesis of multiferroic composites for novel biomedical applications, optimization of electroplated inductors for microelectronic devices; theory of magnetism of Fe-Al alloys; and two advanced analytical approaches for modeling of magnetic materials using Everett integral and the inverse problem approach. This book is addressed to a diverse group of readers with general background in physics or materials science, but it can also benefit specialists in the field of magnetic materials.

How to reference

In order to correctly reference this scholarly work, feel free to copy and paste the following:

Tibor-Adrian Óvári, Nicoleta Lupu and Horia Chiriac (2012). Rapidly Solidified Magnetic Nanowires and Submicron Wires, Advanced Magnetic Materials, Dr. Leszek Malkinski (Ed.), ISBN: 978-953-51-0637-1, InTech, Available from: http://www.intechopen.com/books/advanced-magnetic-materials/rapidly-solidified-magnetic-nanowires-and-submicron-wires

INTECH
open science | open minds

InTech Europe
University Campus STeP Ri
Slavka Krautzeka 83/A
51000 Rijeka, Croatia
Phone: +385 (51) 770 447
Fax: +385 (51) 686 166
www.intechopen.com

InTech China
Unit 405, Office Block, Hotel Equatorial Shanghai
No.65, Yan An Road (West), Shanghai, 200040, China
中国上海市延安西路65号上海国际贵都大饭店办公楼405单元
Phone: +86-21-62489820
Fax: +86-21-62489821

IntechOpen